Chapter 5
Numerical Prediction of the Critical Thrust Force Causing Delamination at the Hole Exit

5.1 Introduction

Delamination at the exit of the hole is considered the most costly damage in the composite structure [1, 4–7, 9–11, 14–21, 22, 23]. This defect leads to a significant loss of the tensile strength and the stiffness of the composite part when it is loaded in compression, shear or fatigue loading [14, 15, 18]. Consequently, this results in a reduction of the loading capacity of the composite part. Several studies have shown that the presence of delamination at the exit side of the hole is mainly due to the axial thrust force developed during the drilling process. This thrust force is mainly related to the interaction between the active part of the cutting tool (cutting edges, chisel edge) and the uncut part of the composite located under the point angle of the drill [5]. However, this thrust force is strongly influenced by the drill diameter, the feed rate of the tool, the nature of material being machined (fibre and resin), the type of web thinning of the tool (point angle, web thickness etc.), and the fibre content [1, 23]. Even drilling at an optimal choice of cutting parameters, the wear of the cutting tool causes an increase in the thrust force which leads to the appearance of delamination at the hole exit.

Two types of models are available in the literature to predict thrust force during drilling. The first one is an empirical model to predict the thrust force as a function of cutting parameters. These empirical models for predicting the thrust forces are similar to those developed in the context of drilling of metallic materials [2, 8, 13]. As a whole, it is based on the identification of the specific cutting pressure of the material to be machined. The second one is an analytical model to predict the critical thrust force responsible for delamination at the exit side of the hole. Beyond this force, there is a high probability of propagation of delamination at the hole exit. These analytical models were inspired by the model developed by Ho-Cheng [5]. Their model development is based on the theory of fracture mechanics, using linear elastic and plate theory. These analytical models are developed from two strong hypotheses. For the first hypothesis, they consider that the critical thrust force is controlled only by the critical energy release rate in mode I (G_{Ic}) of the composite material. For the second assumption, they assume the presence of a

V. Krishnaraj et al., *Drilling of Polymer-Matrix Composites*,
SpringerBriefs in Manufacturing and Surface Engineering,
DOI: 10.1007/978-3-642-38345-8_5, © The Author(s) 2013

circular or elliptical crack near the nominal diameter of the drilled hole. This chapter is composed into two parts. In the first part analytical models available in the literature concerns the prediction of the critical thrust force responsible for delamination at the hole exit during drilling CFRP plates is summarised. In the second part, the elements of a numerical model to predict the critical thrust forces during drilling of composite plate according to the number of plies located under the active part of the drill have been presented. This model is based on analytical models developed by [5, 19, 20] and for isotropic materials [7, 11, 16, 22] for orthotropic materials. In this numerical model, the critical thrust force is controlled by the critical energy release relates in mode I and in mode II of the material to be machined. This represents a step forward compared to the analytical models from the literature which considers only the critical energy release relates in mode I [5, 7, 11, 12, 16, 19, 20, 22]. The originality of the proposed numerical model is the consideration of factors not taken into account by the analytical models. Some of the factors are:

- The influence of the conicity of the drill in the material,
- The presence of a circular crack in the composite located near the chisel edge of the drill,
- The influence of rate of loading induced by the chisel edge and by the principal cutting edges,
- The critical thrust force is controlled by a criterion taking into account the energy release rates in mode I and in mode II of the material concerned.

5.2 Analytical Models from the Literature

5.2.1 Models with the Hypothesis of Isotropic Material

5.2.1.1 Hocheng and Dharan Model (1990)

The first model was developed by Hocheng and Dhahran [5] (Ref. Figure 5.1). During drilling of material, the uncut plies located under the tool (chisel edge) are extruded downwards by the thrust force and undergo elastic deformation. If the resulting stress in the vicinity of the crack tip exceeds a critical value, then the crack propagates. At this point, it is supposed that the force applied corresponds to the critical thrust force.

The assumptions used in this model are:

- The mechanical behaviour of the laminate is considered elastic and isotropic and the delaminated area is supposed symmetrical with respect to the axis of the tool,
- The propagation of delamination at the hole exit is carried out in mode I,

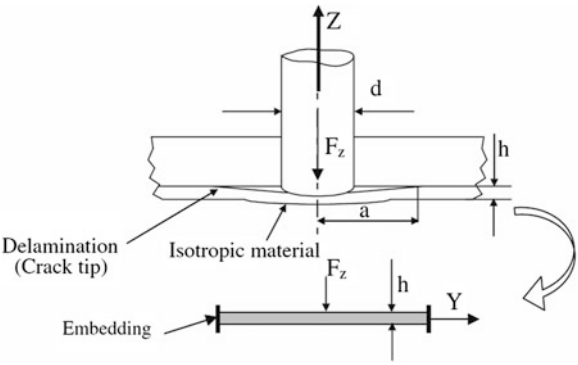

Fig. 5.1 Modeling of the delamination at the exit of the hole according to Ho-Cheng

- The fracture mechanics in the frame of linear elastic is used,
- The crack is considered circular with a radius "a",
- The thrust force of the drill is oriented from the top to the bottom of the plate and its result is applied at the center of the hole,
- The uncut laminate (located under the drill) is subjected to a bending with respect to the hypothesis of small displacements,
- The global bending of the plate is neglected.

The energy balance applied to the structure in the linear elastic is

$$G\pi(2a)\delta a = F_z \partial w - \partial U \tag{5.1}$$

$$G\pi(2a) = F_z \frac{\partial w}{\partial a} - \frac{\partial U}{\partial a} \tag{5.2}$$

with

- U the strain energy of the laminate (J),
- W the local deflection of the part located under the delaminated zone and considered like a plate (mm),
- G the surface energy (J/mm^2),
- Fz the resulting critical thrust force.

Using the plate theory, the authors [5] established a relation to predict the critical thrust force, by considering energy release rate in mode I (G_{Ic}), the elastic mechanical properties of the material (E, υ) and the thickness of the damaged plies (h):

$$F_z = \pi \left[\frac{8 G_{IC} E h^3}{3(1 - \upsilon^2)} \right]^{1/2} \tag{5.3}$$

5.2.1.2 Upadhyay and Lyons Model

Upadhyay et al. [20] introduced two new assumptions compared to the work of Ho-Cheng and Dharan. The first assumption is on the load applied on the area of the uncut plate located under the tool. They made an assumption that the loading is uniformly distributed and not as a concentrated load at the center of the tool. The surface distribution of the loading is considered as circular with radius "a". This radius represents the dimension of the web thickness. In the second hypothesis, the authors consider that under the applied load induced by the drill the bending of the composite plate located under the drill is higher than the thickness of the uncut plies. Therefore, the assumption of large displacements is considered in the model. This assumption is realistic, especially if the area of the composite plate located under the drill is composed of few plies.

By taking these two assumptions into account, the expression of the critical thrust force is given by the Eq. 5.4:

$$F_z = \pi \sqrt{\frac{8G_{IC}Eh^3(1 - 1.464(w_0/h)^2(1 - 0.0488(w_0/h)^2)^2}{3(1 - \nu^2)((1 - 1.708(w_0/h)^2 - 0.107(w_0/h)^4))}} \tag{5.4}$$

with:

- w_0, the maximum deflection at the center of the composite plate (mm),
- E, h, ν and G_{Ic}, are the parameters mentioned in the model similar to Ho Cheng [5].

A comparison of the critical thrust forces (obtained by this model and those given by the model defined by Eq. 5.3) shows only a difference around 12–25 %. The critical thrust forces obtained by the model developed by Hocheng [5] are lower than those measured by experiment and those given by the model Upadhyay et al. [20].

5.2.2 Models with the Hypothesis of Orthotropic Material

The first analytical model to predict the critical thrust force by taking into account of the orthotropy of the composite material was proposed by Jain et al. [6]. Subsequently, many models have been proposed by fellow researchers [11, 16, 22].

Model of Jain-Yang model [7]

$$\mathrm{F_z} = 3\pi \left(\frac{\mathrm{b}}{\mathrm{a}}\right)^{1/4} \sqrt{2\mathrm{G_{IC}D^*}} \tag{5.5}$$

with:

$$D^* = D_{11} + \frac{2(D_{12} + 2D_{66})}{3}\left(\frac{a}{b}\right)^2 + D_{22}\left(\frac{a}{b}\right)^4 \tag{5.6}$$

- D_{ij}, Coefficients of the stiffness matrix of the plate in bending,
- G_{Ic}, the critical energy release rate in mode I,
- a et b, the major and minor radius of the ellipse.

Model of Lachaud et al. [11]

$$F_z = 8.\pi.\left(\frac{G_{IC}.D}{\frac{1}{3} - \frac{D'}{8.D}}\right)^{1/2} \tag{5.7}$$

with:

- G_{Ic} the critical energy release rate in mode I,

$$D = \frac{1}{8}(3D_{11} + 2D_{12} + 4D_{66} + 3D_{22}), \tag{5.8}$$

$$D' = \frac{D_{11} + D_{22}}{2} + \frac{D_{12} + D_{66}}{3}, \tag{5.9}$$

D_{ij}, Coefficients of the stiffness matrix of the plate in bending.

Model of Zhang et al. [22]

$$F_z = \left(\frac{\pi.G_{IC}}{\zeta(C_3 - K)}\right)^{1/2} \tag{5.10}$$

with:

- G_{Ic}, the critical energy release rate in mode I,
- K and C_3, constants dependent on the mechanical characteristics of the composite plate located under the drill.

However, the difference between the numerical model to predict the critical thrust force proposed in this chapter and all analytical models presented above is summarized in the following points:

- the point tool geometry (chisel edge, point angle and cutting length),
- the presence of a crack in the vicinity of the chisel edge of the tool and not near the nominal diameter of the tool,
- the influence of the rate of loading induced by the principal cutting edges and the chisel edge separately,

- the critical thrust force is controlled by a criterion taking into account the critical energy release rate in mode I and in mode II of the composite material,
- the energy of deformation by shear loading.

5.3 Experimental Procedure

Within this study, two types of UD prepreg in carbon/epoxy are used. These raw materials of laminated structures are provided by Hexcel composites and are referenced respectively under, Hexply T2H 268 150 EH25 NS 35 % (noted T2H-EH25) with a 59 % fibre content and a 0.25 mm thick ply and Hexply T700GC 268 M21 34 % (noted T700-M21) with a 58 % fibre content and a 0.26 mm thick ply. Those two products are fairly equivalent from the mechanical properties viewpoint. However, material T700-M21 differs through the presence of 20 μm diameter thermoplastic nodules which represent about 13 % matrix mass rate in the prepreg. These nodules are supposed to improve damage tolerance by initiating a crack network at the interply then controlling the crack propagation within the laminate. The energy release rates of this material in mode I and II increase in comparison with those of T2H-EH25 laminate. The specimens for test present a quasi-isotropic stacking sequence featuring 16 plies $[90^\circ/-45^\circ/0^\circ/+45^\circ]_{2s}$. The drilling of a blind hole is carried out using a CNC machine. In order to avoid delamination while blind-hole machining, the plate to be drilled is supported on its lower face by means of a wood plate. Moreover, the machining parameters are chosen so as to avoid delamination between plies. The machining parameters are based on a small feed rate (the tool feed rate as well as the rotating speed are respectively, 0.001 mm/rev and 1,500 rev/min). The tool is a tungsten carbon micro grain with grade K20 and the principal characteristics of the tool are: (a) Point angle of 118°, (b) Diameter of 4.8 mm and (c) helix angle of 15°. The visual inspection of these blind holes has revealed no delamination or resin crack. We have mentioned in the previous chapters that, the feed rate is the cutting parameter which has a greater influence on the thrust force during drilling with a twist drill, for this reason in this study the influence of the cutting speed on the thrust force, is not taken into account.

The validation of this numerical model is conducted with quasi-static punching tests. The latter are carried out on a standard tensile testing machine INSTRON. The axial load is applied using a twist drill (with a 4.8 mm diameter) which moves in translation in the blind hole. The values of the critical energy release rates in mode I (GIc) and mode II (GIIc) for 0°/45° interface of two studied materials result from the fracture mechanics tests carried out in our laboratory. These tests are performed in accordance with the standard (NF ISO 15024) (Fig. 5.2).

The method of determination of the energy release is based on double cantilever beam (DCB) test. The values obtained GIc and GIIc are in good agreement with the values provided by Hexcel composites. The principal information composed the proposed model are given below.

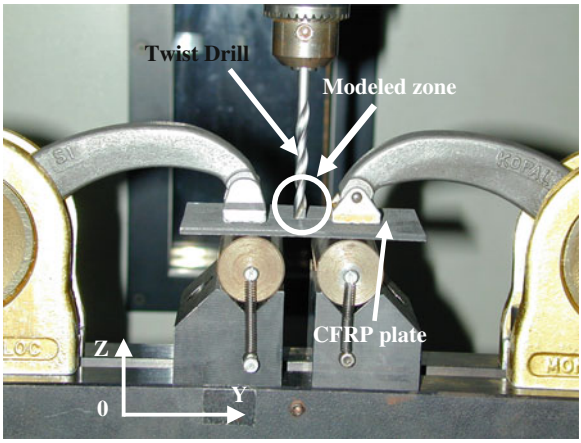

Fig. 5.2 Experimental device for the punching tests

5.4 Numerical Modelling

The numerical model suggested has the advantage of taking into account various aspects. Among them it is noticed that: (a) the consideration of the strain due to the shear forces thanks to the use of an adapted finite element available in the software library of SAMCEF FE code (finite element of type 11).

(b) the second aspect corresponds to the influence of the drill point angle in the material and enables us to represent on the one hand, the presence of a crack at the level of the chisel edge and on the other hand, the influence of the loading distribution on the chisel edge and the principal edges of cut (lips of drill). The resulting thrust force Fz can be decomposed into two components Fz1 and Fz2 (Ref. Figure 5.3), with F_{z1} as the thrust force induced by the contact of the cutting lips with the laminate and F_{z2} as the force corresponding to the contact of the chisel edge with the laminate ($Fz = 2F_{z1} + F_{z2}$). The part of the machined structure is modelled like a volume of circular geometry of external radius Re and

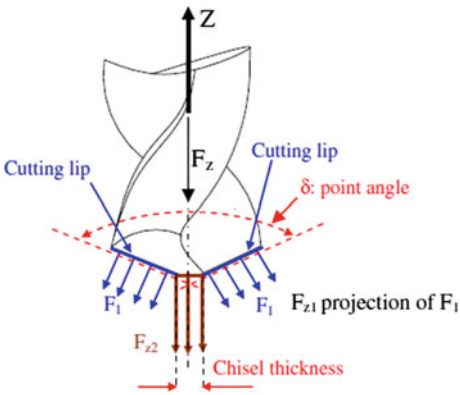

Fig. 5.3 Thrust force induced by the principal cutting edge and the chisel edge

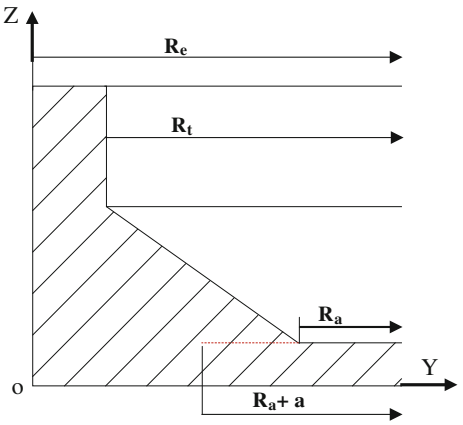

Fig. 5.4 Schematic view of the modelled zone

internal radius R_t (considering that Rt is the nominal drilled hole radius). Figure 5.4 is a schematization of the system section seen in the (YZ) plane. Ra and e respectively represent the chisel edge radius and the thickness of the non-machined plies which are located under the drill chisel edge.

5.4.1 Description of the Numerical Model and Boundary Conditions

Figure 5.5 represents the finite element model of the quasi-isotropic laminate drilling in carbon epoxy. In this modeling, the finite element used is of volumic isoparametric type with degree 2 which is available in the software library of SAMCEF FE code. The interface nodes are located at the middle of the top nodes. The calculation is carried out within a linear static hypothesis with the composite volume assumption. The conditions with imposed boundary correspond to an embedding on the circumference of the hole (of radius Re). A part of the loading is according to the (oZ) direction and is applied on the nodes of the surface generated by the chisel edge at the time of its rotation. The other part of the loading is applied to the conical periphery of the drill (Ref. Figure 5.4). For a crack located on the level of the chisel edge diameter, the principle of determination of the critical thrust force Fz—according to the number of plies under the drill—is based on the calculation of the energy release rate in mode I and mode II. The leading edge of the crack is circular and of radius (Ra + a). The critical value of the thrust force Fz can be obtained if the following energy criterion is checked:

$$(G_I/G_{IC})^{\alpha} + (G_{II}/G_{IIC})^{\alpha} = 1 \tag{5.11}$$

The choice of distribution of the loading quantity (F_{z1} coming through the chisel edge, F_{z2} coming through the cutting lips) is based on literature [8]. The

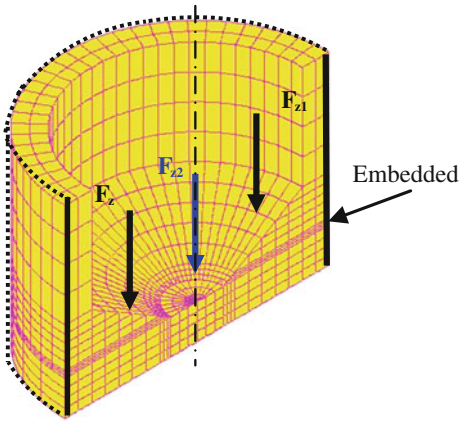

Fig. 5.5 Mesh and boundary condition of the modeled zone

acquisition of thrust forces was carried out with the help of a load sensor of KISTLER type. This identification process was divided into two parts. In the first one, the authors measure the thrust force F_z. In the second one, they make a pilot-hole whose diameter is equal to the dimension of the chisel edge ($2R_a$), then on the same previously-drilled laminate, they machine a hole of diameter ($2R_t$) followed by a measurement of the overall contribution of the two main cutting lips. Figure 5.6 represents the result of this study: for small feed into the material (around 7 mm/min), the part of the thrust force F_{z2} generated by the chisel edge accounts to 40–50 % of the total thrust force F_z.

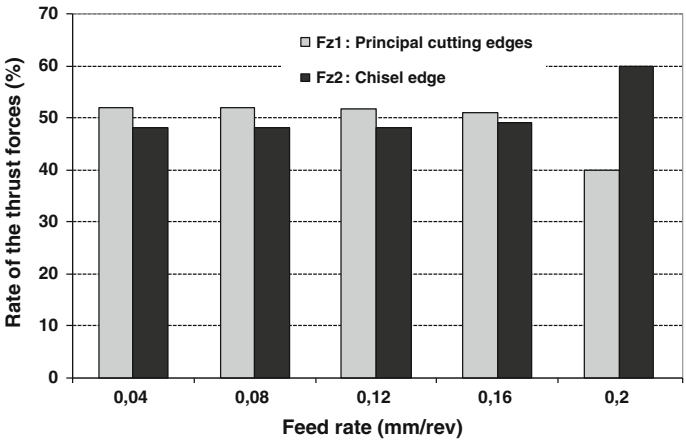

Fig. 5.6 Evolution of the thurst force induced by the principal cutting edge and that induced by the chisel edge during drilling of metallic material using twist drill

This quantitative identification is obtained using dynamic tests (at 7 mm/min tool feed) and this identification is supposed not to change a lot if the tests are carried out in quasi-static context (at 1 mm/min tool feed). As the numerical model proposed is developed in a quasi-static context, validating this model in the same situation seems more relevant.

5.5 Resultants and Discussion

5.5.1 Study of the Influence of Mesh

Firstly, how the choice of the outer radius value (R_e) influences the energy release rate in mode I is studied. To do so, the total number of elements is fixed at 3,480 elements, the dimension of the pre-crack is equal to 0.5 mm and the loading effort on the chisel edge F_{z2} represents 40 % of the total thrust force F_z. Figure 5.7 illustrates G_I variation according to R_e in the case of three plies under the drill and for the two materials under study. The energy release rate in mode I (G_I) is seen as being globally constant for an embedding radius varying from 2.6 to 3.1 mm.

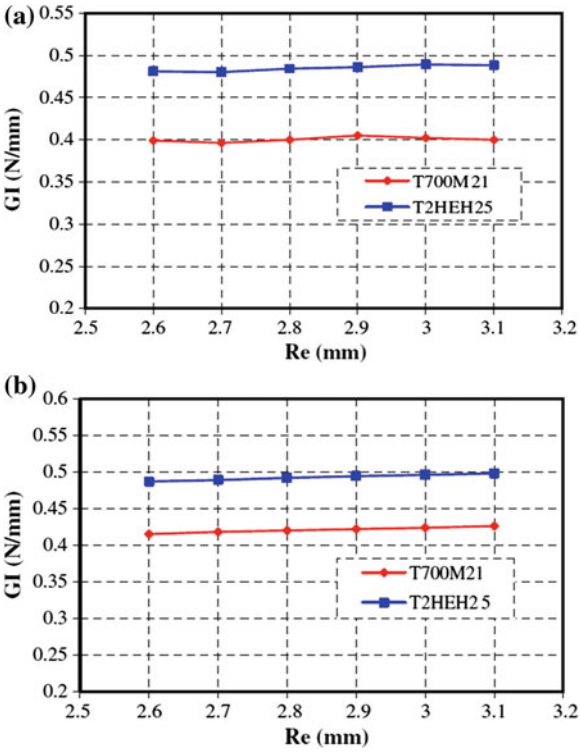

Fig. 5.7 Study of the influence of embedding radius Re on the numerical results with two plies under the drill; boundary conditions: Fz = 500 N, a = 0.5 mm when Fz2 = 40 % Fz. **a** Three plies under the tool. **b** Two plies under the tool

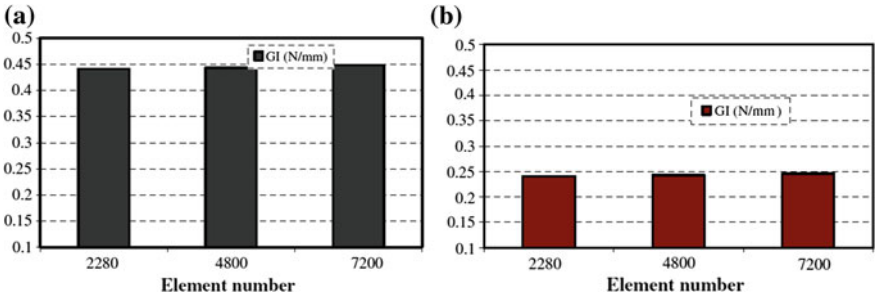

Fig. 5.8 Study of the influence of the total number of elements on the numerical results; boundary conditions. **a** Material T700-M21, Fz = 540 N, a = 0.5 mm with three plies under the drill. **b** Material T2H-EH25, Fz = 230 N, a = 0.5 mm with three plies under the drill

Moreover, in the case of two plies under the drill, it is noticed that the variation of the embedding radius does not lead to a significant variation of the energy release rate in mode I for the two materials (Ref. Figure 5.7a). The value chosen for this study is 2.9 mm. Secondly, the influence of the number of elements on the results is examined. Thus, a 2.9 mm radius Re and a 0.5 mm pre-crack are chosen. Figure 5.8 shows that the use of a number of elements from 2,280 to 7,200 elements has led the energy release rate in mode I to increase by 2 %. This involves T2H-EH25 material. In brief, the total number of elements used in the model has a very little influence on the global thrust force value F_z whatever the material studied (Ref. Fig. 5.8a and b). The final part is devoted to the influence of the pre-crack length "a" on the thrust force "F_z". The total number of elements as well as the outside radius of the model is thus respectively fixed at 4,800 and 2.9 mm. Figure 5.9 features how the pre-crack length influences the global thrust force F_z with three plies under the drill and for the two materials studied: when the pre-crack length varies from 0.25 to 0.8 mm, the thrust force is quasi-constant. Similar observations can be made with two plies under the drill. The numerical results exposed in this study are obtained with a mesh of 4,800 elements, a 2.9 mm embedding radius and a 0.3 mm pre-crack length. It has been checked that the

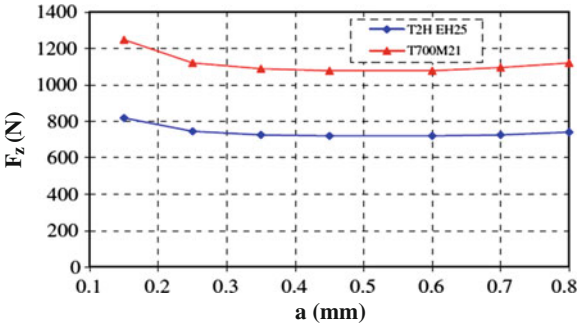

Fig. 5.9 Influence of the crack length (a) on the thrust force (Fz); boundary conditions: three plies under the drill, materials T700-M21 and T2H-EH25, Fz2 = 40 % Fz

fixed parameters (Re, a and the number of elements) are not dependent on the type of the stacking sequence under study.

5.5.2 Macro Scale Analysis

Figure 5.10a represents a comparison experiment/numerical calculation of the thrust forces Fz (for a carbon/epoxy plate of T2H-EH25 material, a 4 mm thickness and a quasi-isotropic stacking sequence of type $[90/+45/0/45]_{2s}$). If the loading taken by the chisel edge drill represents 50 % of the total loading, it is noted that the relative difference between the results provided by the numerical model and those given by the experiment is important (around 50 %). This is checked as soon as the number of the plies under the drill is higher than two. If the loading taken by the chisel edge represents 40 % of the total loading, the results of the numerical model corroborate the experimental measurements. In this case of loading, whatever the number of plies under the drill is, the relative variation remains under 11 %.

However, for material T700-M21 (and when the loading share taken by the chisel edge is 40 %), Fig. 5.10b shows a good correlation calculation/test if the

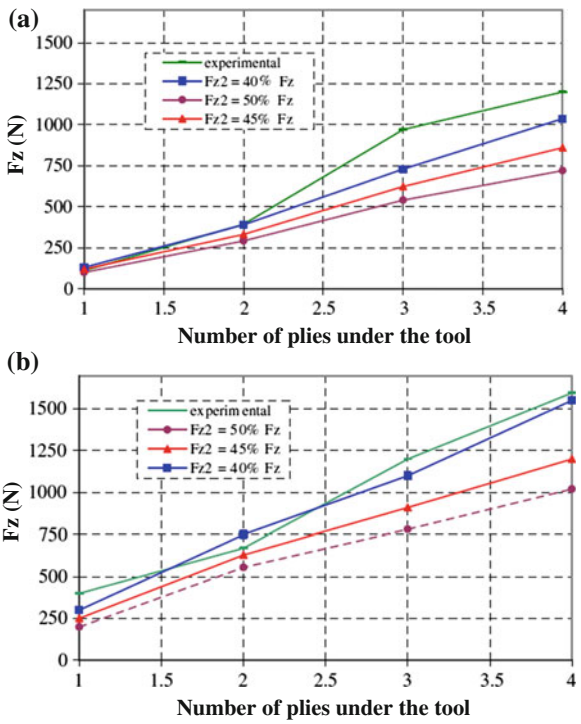

Fig. 5.10 Comparison between the experimental and the numerical critical thrust forces responsible of delamination (**a**) Material T2H-EH25 and (**b**) Material T700-M21

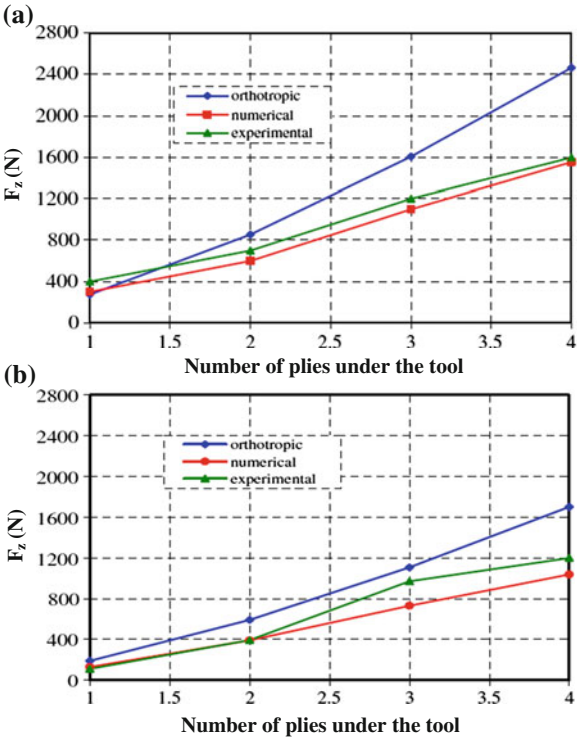

Fig. 5.11 Numerical model/experiment/model (orthotropic) correlation; with the conditions: $F_{z2} = 40$ % of the total Fz. (**a**) T700-M21 material and (**b**) T2H-EH25 Material

number of plies is over one. Moreover, the critical thrust force calculated for material T700-M21 is higher than those calculated for material T2H-EH25 (and that for all numbers of plies under the drill). This can be explained by the presence of thermoplastic nodules in the T700-M21 material which increases the values of energy release rates in mode I and II and therefore the critical outside load which is responsible for the crack spreading.

In Fig. 5.10, the correlation numerical model/experiment/analytical model is presented. The assumption of orthotropic material [11] is considered for the two types of materials under study. For this numerical calculation, the retained distribution of the loading corresponds to a resumption of 40 % by the drill chisel edge and of 60 % by the drill lips. According to Fig. 5.11a, a good correlation is observed between the numerical model and the experiment. The analytical model overestimates the critical efforts responsible for the delamination between the plies whatever the material under study may be. As an example, in the case of material T700-M21 and four plies under the drill, the maximum relative variation registered between the experiment and the analytical model is 42 %. However, in the same situation, the relative difference between the experiment and the numerical model is only 3 %. Similar conclusions are obtained in the case of material T2H-EH25 (Ref. Fig. 5.11b).

5.5.3 Meso Scale Analysis

In Figs. 5.12 and 5.13, the application of the Tsai–Wu criterion is presented for the two studied materials respectively, T2H-EH25 and T700-M21. That corresponds to a situation of calculation in which there are three plies under the chisel edge of the drill and the energy criterion described in the Eq. (5.11) is checked. The Tsai–Wu criterion announces a damage risk in the zone close to the drill chisel edge as well as at the level of the tip crack. The frontiers of the zones drawn with a discontinuous line on these cartographies represent the print of the damage propagation in the vicinity of the crack between plies under the applied load. This cracking propagation announces some delaminated zones which are qualitatively of the same shape as those observed through radiography [3, 23]. In the work of Zitoune et al. [23] drilling of the laminate (without back up) is carried out with a

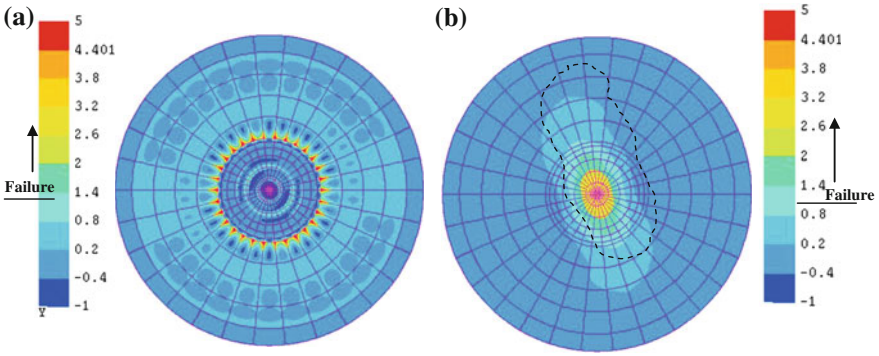

Fig. 5.12 Tsai–Wu criterion for the T2H-EH25 material; (**a**) *top* view, (**b**) *underside* view, machining conditions: three plies under the drill and $F_z = 750$ N

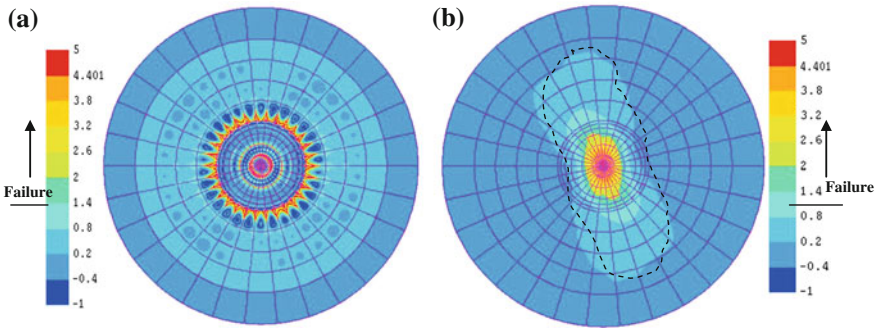

Fig. 5.13 Tsai–Wu criterion for the T700-M21 material; (**a**) *top* view, (**b**) *underside* view, machining conditions: three plies under the drill and $F_z = 1150$ N

high feed rate (1 mm/rev) and the resulting thrust force (1,000 N) is of the same scale as the value calculated in this study. It can be noticed that a feed rate lesser to 1 mm/rev (for example 0.02 mm/rev) implies that the delamination at the exit of the hole widespread within the ply and not in inter-ply zones.

SEM images of the Fig. 5.14 show the presence of delamination at the 90/+ 45 interface in the vicinity of the drill chisel edge. This phenomenon is observed for the various numbers of plies under the drill. That consolidates the assumption of the crack presence at the level of the drill chisel edge. The presence of caulking

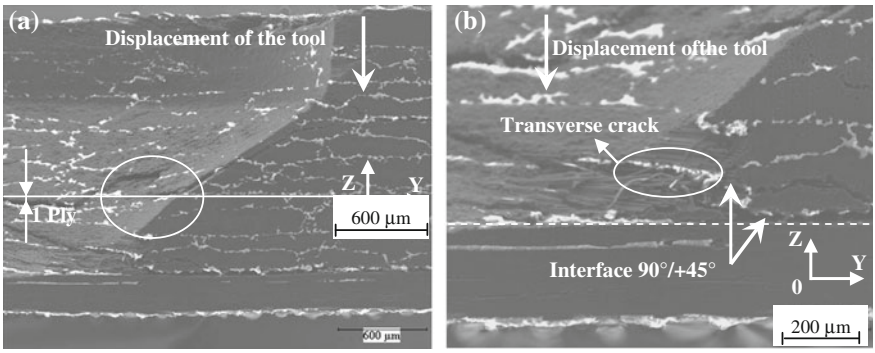

Fig. 5.14 SEM micrographs of the state of the hole after the punching test of the laminate T700-M21 in half cross-section; test conditions: one ply under the drill, (**a**) ×150 magnification and (**b**) ×300 magnification

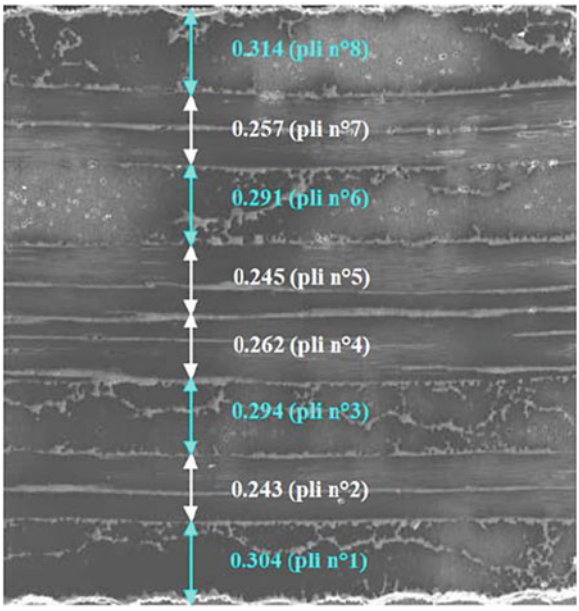

Fig. 5.15 SEM picture of the thickness of composite T700-M21 of stacking sequence $[0/90]_{2s}$ and manufactured in autoclave

can also be observed around the zone of tool/laminated contact due to the tool advance. These caulking zones are certainly the place of an intense pressure and friction between the tool face and the laminate. This friction phenomenon should be taken into account in a modelling.

From these pictures it is observed that, it is difficult to control with precision the position of the chisel edge or the extremity of the drill in the materials. This difficulty is linked the variability of the plies thickness of the composite materials after the setup of curing. In the Fig. 5.15, we represent an SEM analysis of specimens with $[0°/90°]_{8s}$ after the setup of polishing. It is noticed that, the measured thickness of the plies varies from 0.245 to 0.314 mm. These values represent 20 % of gap compared to the theoretical value of the ply thickness mentioned by Hexcel composite.

5.6 Summary

For the analysis of the drilling conditions of long-fibre composite structures, the numerical model that is proposed is based on the fracture mechanics. This modeling enables to restore the critical thrust forces responsible for the formation of the defect at the exit of the hole and for a different number of plies under the drill chisel edge. The validation of this numerical model is carried out thanks to quasi-static punching tests on two types of carbon/epoxy materials. The right correlation has been noticed between the numerically calculated efforts and those which were experimentally obtained. The maximum variation registered is about 15 %. This gap can be related to mechanical proprieties used in the model that are affected by the variability of the ply thickness after the curing phase. A confrontation between the critical thrust forces, numerically obtained, and those obtained thanks to the analytical model is carried out. The proposed model, validated on two types of carbon epoxy laminated, can also be used for other composite materials from UD prepreg. However, its validity has not been fully proved on composite material made of woven fabric. Following the numerical study of the critical thrust force, it would be interesting to exploit them to the most in order to identify the critical feed rates so as to avoid delamination during the drilling phase. This phase can be achieved thanks to the empirical patterns in the literature which give the thrust force according to the tool feed rate. It has been shown that the beginning of the damage due to the tool displacement is located around the chisel edge and not around the nominal diameter. Thus we proposed the development of an analytical model which predicts the critical thrust force by taking into account a crack presence in the vicinity of the chisel edge. The integration of shear effects in that analytical model is also planned.

References

1. Chen WC (1997) Some experimental investigation in the drilling of the carbon fiber-reinforced plastics (CFRP) composite laminates. Int J Mach Tools Manuf 37:1097–1108
2. Dallas DB (1976) Tool and manufacturing engineers handbook. Drilling, reaming and related operation, Chapter 3, pp 1–99
3. Gaitonde VN, Karnik SR, Campos Rubio J, Esteves Correia A, Abrao AM, Davim JP (2008) Analysis of parametric influence on delamination in high-speed drilling of carbon fiber reinforced plastic composites. J Mater Process Technol 203:431–438
4. Hamdoun Z, Guillaumat L, Lataillade J-L (2004) Influence of the drilling on the fatigue behaviour on the carbon/epoxy laminates. ECCM 11 1:301–302
5. Hocheng H, Dharan CKH (1990) Delamination during drilling in composite laminates. J Eng Ind 112:236–239 Transactions of ASME
6. Jain S, Yang DCH (1993) Effects of feedrate and chisel edge on delamination in composites drilling. J Eng Ind 115:398–405 Transactions of ASME
7. Jain S, Yang DCH (1994) Delamination free drilling of composites laminates. J Eng Ind 116:475–481 (Transaction ASME)
8. Kang TH, Carless JW (1971) Cutting force analysis in drilling, ASME Technical paper MR71-170
9. Kashaba UA (2004) Delamination in drilling GRP- thermoset composites. Compos Struct 63:313–327
10. Krishnamoorthy A, Rajendra BS, Palanikumar K (2011) Delamination prediction in drilling of CFRP composites using artificial neural network. J Eng Sci Technol 6(2):191–203
11. Lachaud F, Piquet R, Collombet F, Surcin L (2001) Drilling of composite structures. Compos Struct 52:511–516
12. Lévêque D (1998) Analyse de la Tenue au Délaminage des Composites Stratifiés: Identification d'un Modèle d'Interface Interlaminaire". Thèse de Doctorat de l'Ecole Normale Supérieure de Cachan
13. Montgomery DC (2001) Design and analysis of experiments. Wiley, New York
14. Murphy C, Byrne G, Gilchrist MD (2002) The performance of coating tungsten carbide drills when machining carbon fiber reinforced epoxy composite materials. Inst Mech Eng 216 Part B:143–152
15. Person E, Eriksson I, Zackrisson L (1997) Effects of hole machining defects on strength and fatigue life of composite laminates. Composites Part A Appl Sci Manuf 28(2):141–151
16. Sadat AB (1996) Prediction of delamination load in drilling of graphite/epoxy composites. Eng Syst Design Anal 3:21–27
17. Shaw MC (2005) Metal cutting principles, 2nd edn. Oxford university press, New York
18. Singh I, Bhatnagar N, Viswanath P (2008) Drilling of unidirectional glass fiber reinforced plastics: Experimental and finite element study. Mater Des 29:546–553
19. Tsao CC, Hocheng H (2008) Evaluation of thrust force and surface roughness in drilling composite material using Taguchi analysis and neural network. J Mater Process Technol 203:342–348
20. Upadhyay PC, Lyons JS (1999) On the evaluation of critical thrust for delamination-free drilling of composite laminates. J Reinf Plast Compos 18(14):1287–1303
21. Campos Rubio J, Abrao AM, Faria PE, Esteves Correia A, Davim JP (208) Effects of high speed in the drilling of the delamination factor. Int J Mac Tools Manuf 48:715–720
22. Zhang LB, Wang LJ, Liu XY (2001) Mechanical model for predicting critical thrust forces in drilling composite laminates. Proc I MECH E Part B J Eng Manuf 215:135–146
23. Zitoune R, Krishnaraj V, Collombet F (2010) Study of drilling of composite material and aluminium stack. Compos Struct 92(5):1246–1255